IEEE/CSC & ESAS European Superconductivity News Forum (ESNF) No. 22 October/November 2012..
The published version of this preprint appeared in IEEE Transactions on Applied Superconductivity 23, 5500206 (June 2013).

Verification Testing for a 1 MVA 3-Phase Demonstration Transformer Using 2G-HTS Roebel Cable

Neil. D. Glasson, Mike. P. Staines, Zhenan Jiang, and Nathan. S. Allpress

***Abstract*—We present results from testing to verify performance of major sub-system components for a 1 MVA 3-phase transformer demonstration project. The transformer utilizes a 15 strand Roebel cable for the low voltage windings and 4mm wide superconductor for the high voltage windings. Both windings use YBCO conductor. The winding assemblies are housed in three individual vacuum insulated glass-fiber composite cryostats and are cooled by circulated liquid nitrogen, sub-cooled to a target operating temperature of 70K. Results from thermal insulation performance tests on a sample composite cryostat are presented. AC loss test results of a low voltage winding assembly are also presented. The Roebel cable is proven to exhibit low AC loss operation at high current. We conclude that AC loss is not a fundamental obstacle to HTS transformer commercialization.**

***Index Terms*—Cables, Cryogenics, Superconducting Transformers.**

I. Introduction

ROEBEL CABLE has been identified as a most promising technology for producing a compact superconducting winding cable with high current carrying capacity, excellent current sharing and good AC loss performance [1],[2],[3]. The capability to manufacture commercially useful lengths of HTS Roebel cable (from 2G-HTS conductor) has been developed over recent years by General Cable Superconductors [4].

One challenging application that would take advantage of the positive attributes of HTS Roebel cable is an HTS transformer. HTS transformers promise high efficiency, fault current limiting, reduced size and weight, improved environmental and fire safety performance, and increased operational lifetime when compared to conventional equipment [5]. One of the major challenges to successful implementation of a commercially viable HTS transformer is the high cost of the cooling system [6]. In the current project, we aim to demonstrate a Roebel cable based HTS transformer with parameters as described in Table I. This grid-connected prototype aims to demonstrate the utility of HTS Roebel cable as an effective means of implementing a stable high current winding with low AC loss, thus minimizing the heat load on the cooling system (and therefore the cooling system capital and operating costs).

In the current work, we aim to experimentally quantify two of the key contributors to heat load on the cryogenic system – the cryostat insulation performance and the AC loss performance of the Roebel cable winding.

TABLE I
TRANSFORMER DESIGN PARAMETERS

Parameter	Value
Primary Voltage	11,000 V
Secondary Voltage	415 V
Max. Operating Temperature	70 K, liquid nitrogen cooling
Target Rating	1 MVA
Primary Connection	Delta
Secondary Connection	Wye
LV Winding	20 turns 15/5 YBCO Roebel cable
LV Rated winding current	1390 A rms
HV Winding	918 turns of 4 mm YBCO wire
HV Rated winding current	30 A rms

II. Test Description

The key features of the transformer cryostat and the low voltage (LV) winding are presented below, along with a description of the experiments undertaken:

A. Cryostat – heat leak determination

The transformer cryostat is comprised of an assembly of warm and cold shells fabricated from glass-fiber composite material (of a formulation similar to G10). There is a warm bore through the cryostat so that the core of the transformer can remain outside the cryogenic region. It is impractical to have the core cold due to the cooling penalty on the significant no-load losses from the core. The cold shell is designed to contain an internal pressure of 3 bar (gauge) to allow for overpressure during venting in the event of a malfunction.

Manuscript received October 9, 2012.

N. Glasson, M. Staines, Z. Jiang and N. Allpress are with Industrial Research Limited, Lower Hutt 5040, New Zealand (e-mail:n.glasson@irl.cri.nz).

The published version of this preprint appeared in IEEE Transactions on Applied Superconductivity 23, 5500206 (June 2013).

The insulation space between the cold and warm shells is filled with glass microspheres and evacuated to better than 10^{-2} mbar. Glass microspheres were selected for the vacuum space insulation medium as they offer good insulation performance at modest vacuum and are relatively cheap and easy to install [7]. They also offer the considerable advantage over MLI in that they are electrically insulating. MLI can offer better insulation performance but it requires much better vacuum and great care must be taken to avoid continuous electrically conductive turns of MLI encircling the core – acting as shorted electrical turns on the transformer.

A transformer cryostat is shown in Fig 1. Note that the central axis of the core bore is eccentric with the outer shell. This allows for a more compact transformer, while still offering sufficient internal space to accommodate the windings and electrical connections. Minimizing the cryostat size in this way has the added advantage that the surface area of the walls (and therefore the heat leak through the walls) is also minimized.

Fig. 1. Composite transformer cryostat for one phase – shown without lid. Note the eccentric central tube.

The lid for the cryostat is a solid G10 plate secured to the cryostat with stainless steel fasteners. A thick, medium density expanded polyurethane foam slab is fitted to the underside of the lid to insulate the space between the lid and the liquid nitrogen. We have been unable to establish a satisfactory static vacuum in the vacuum space of the composite cryostat. The vacuum space will therefore be continually pumped to maintain a suitable vacuum. Others have reached a similar conclusion - that it is very challenging to construct composite cryostats that can contain a good static vacuum in the insulation space [8].

In order to more conveniently test construction methods and performance of a composite cryostat, we started with a smaller and simpler cryostat as depicted in Fig. 2. This small test cryostat was used for the thermal performance testing presented here.

Fig. 2. Small test cryostat on scales undergoing a test. Polyurethane foam encases the fill port and the vent tube to limit heat leak via these openings.

The small test cryostat was placed on a set of scales so that the mass of liquid nitrogen could be monitored as it boiled off - Fig. [2]. A vacuum pump was attached to the insulation vacuum port. A vented lid was fitted that mimics the lid configuration of the transformer cryostat. The design operating temperature of the transformer is 70 K. At close to atmospheric pressure, this means that there will be no gas space beneath the foam insulation. In this test it was reasoned that having a gas space between the foam insulation and the liquid nitrogen is not desirable because it does not represent the eventual transformer configuration, and may therefore give a false indication of thermal performance. It was expected that a good determination could be made of the boil-off rate at the maximum fill level - with the liquid nitrogen in intimate contact with the foam plug.

B. Roebel Cable Winding Assembly – AC loss testing

The Roebel Cable winding was assembled onto a composite former as a single layer solenoid winding. The cable is restrained in a shallow machined helical groove to maintain

separation between turns. The cable is terminated onto copper contacts by soldering. The Roebel cable winding assembly is designed to be suspended by studs from the cryostat lid that fasten into a flange which is integral with the cable former. The cable winding in progress is depicted in Fig. 3. The actual transformer LV winding was used as the basis for a test transformer assembly to carry out AC loss measurements focused on the AC loss in the LV winding alone. The LV winding is expected to have the greatest impact on the transformer efficiency – the rated current amplitude is about 80% of the predicted cable critical current at 70 K [9], compared with about 25% for the HV winding.

For the AC loss measurement, the LV winding was short circuited and the winding was energized with a copper HV winding. The test transformer assembly was without iron core for convenience, with both windings immersed in liquid nitrogen, and to avoid accounting for core losses. This approach was taken to mimic as closely as possible the LV winding as it will be inside the final transformer assembly. AC loss measurements on the LV winding are thus expected to approximate closely the losses in the assembled transformer.

The copper HV winding was wound as a 1330 turn solenoid winding using Litz wire. One strand of the 35 strand Litz wire was used to sense induced voltage in the HV winding – thereby allowing the HV pickup winding to measure power delivered by the HV winding without being obscured by the ohmic loss in the winding[15], about 500 W at rated current. A schematic of the circuit for AC loss measurement is shown in Fig. 4. The power dissipated in the LV winding is the difference between the power delivered to the secondary circuit and the power dissipated in the shorting resistor:

$$P_{SC} = V_1 \cdot I_1 - V_S \cdot I_2 \qquad (1)$$

The loss in the LV winding cannot be measured directly from contacts on the winding because a significant fraction of the loss is due to magnetization currents, predominantly in the end turns, which are induced by the radial field from both primary and secondary windings.

At low current, particularly, the winding loss is the difference between two relatively large numbers; measurements of the voltage - current pairs were made using lock-in amplifiers with care taken to keep phase shift errors below 0.01°. Currents I_1 and I_2 were measured using Rogowski coils which were calibrated together against a standard resistor. The large inductive voltage from the HV pickup coil, approaching 1kV depending on frequency, was attenuated and an inductive component derived from the primary current Rogowski coil subtracted using an analogue summing amplifier before the lock-in amplifier.

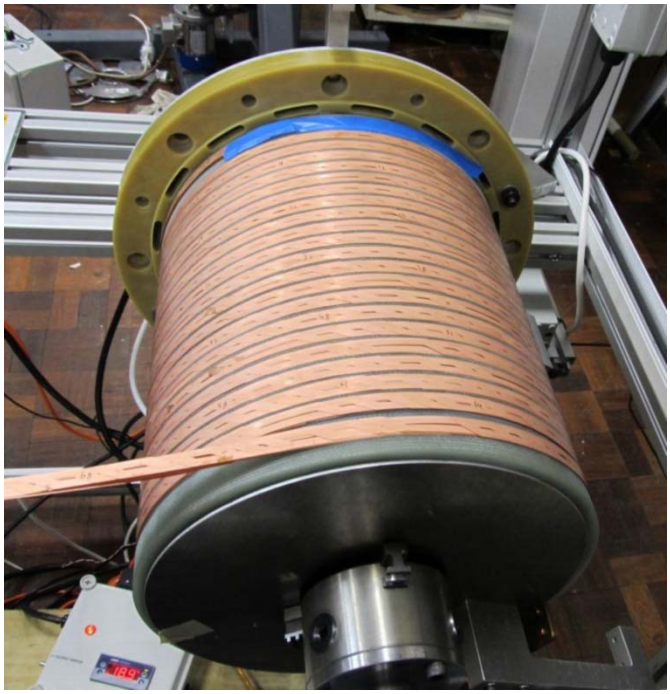

Fig. 3. Low voltage Roebel Cable winding in progress.

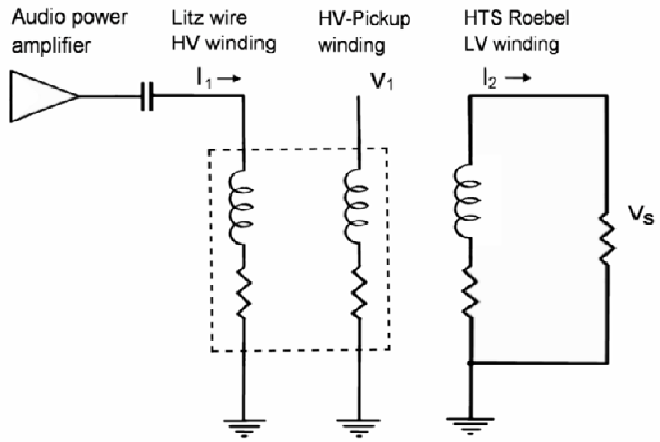

Fig. 4. AC loss measurement - conceptual circuit schematic.

III. Results, Analysis and Discussion

A. Cryostat

The small cryostat boil-off test results are as described in Fig. 5. The mass trend line was differentiated and factored by the heat of vaporisation of nitrogen to establish the corresponding heat leak rate in Watts. The main result of interest is the peak heat leak rate of 18 W (at the start of the test). This corresponds with the heat leak when liquid nitrogen is in intimate contact with the insulating polyurethane foam layer beneath the lid – a condition that most closely matches the operating condition of the transformer cryostat.

The published version of this preprint appeared in IEEE Transactions on Applied Superconductivity 23, 5500206 (June 2013).

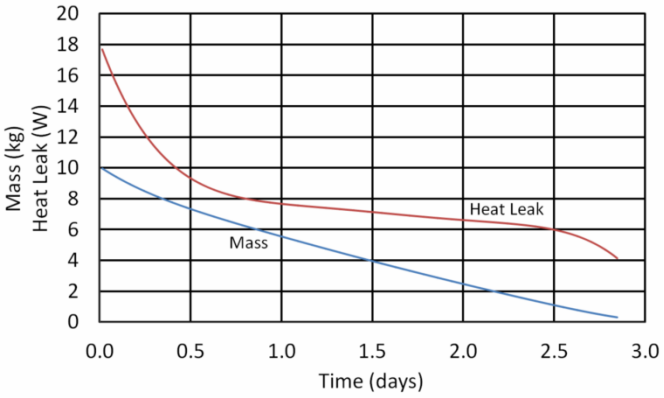

Fig. 5. Liquid nitrogen boil-off test results for small test cryostat.

It is interesting to note that the heat leak rate drops rapidly as the liquid level falls. This is due to a combination of the additional thermal insulation offered by the gas layer and the longer thermal conduction path down the cold shell walls to the liquid. One conclusion from this result is that a significant insulation performance advantage may be had by designing a cryostat with some gas space additional to any foam insulation beneath a lid. Beyond a threshold (in this geometry about 50mm gas space) the improvement in insulation performance diminishes. It should be noted that an insulating gas space beneath the foam layer is not possible with our transformer design because we will be operating with the nitrogen sub-cooled to 70K at close to atmospheric pressure. This is necessary to achieve the electrical rating target for the transformer and is desirable for maintaining reliable dielectric and heat transfer performance [9]. The temperature profile through the foam insulation will mean that there will be a liquid/gas interface somewhere between the bottom and the top of the foam insulation (in any small gaps around penetrations in the foam insulation).

The thermal performance of the small test cryostat was also calculated by analytical means. The system was modelled to determine the heat leak via the three available paths:

1) down through the lid and foam layer (Lid)
2) through the vacuum insulated space (Shell), and
3) down through the inner G10 cold shell (Wall).

Apparent thermal conductivity properties of the materials used in the cryostat are shown in Table II. This data is derived from published sources [10],[11] and describes the apparent thermal conductivity over the nominal temperature range 70K to 300K.

The calculated heat leak from the three leak paths is represented in Fig. 6. This shows that for the small cryostat construction, the dominant heat leak is the conduction path down the cryostat wall. The contribution through the glass microsphere insulation is relatively minor. Note that the measured heat leak of 18 W is 22% lower than the calculated total heat leak of 23.2 W. This difference is possibly due to additional thermal resistance in both fluid boundary layers and at solid-solid interfaces – neither of which were allowed for in the calculation.

TABLE II
APPARENT THERMAL CONDUCTIVITY OF CRYOSTAT MATERIALS

Material	Apparent Thermal Conductivity (mW/m•K)
G10 (warp)	630
G10 (normal)	430
Polyurethane Foam	27
Glass Microspheres	0.83

A similar calculation was applied to the design for the much larger transformer cryostat. Results from this calculation are represented in Fig. 7. The proportions of heat leak through the various paths are markedly different, reflecting the differences between the two geometries. The vacuum and glass microsphere insulated walls in particular have much larger area (> 600% larger) and the insulation cavity is thinner on the transformer cryostat.

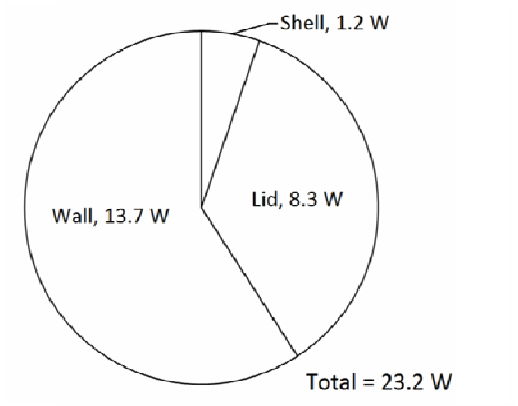

Fig. 6. Calculated heat leak into small cryostat.

It is expected that subsequent planned testing of the transformer cryostat (repeating the test done on the small cryostat) will confirm that the calculated heat leak is an over-estimate of the actual heat leak into the cryostat.

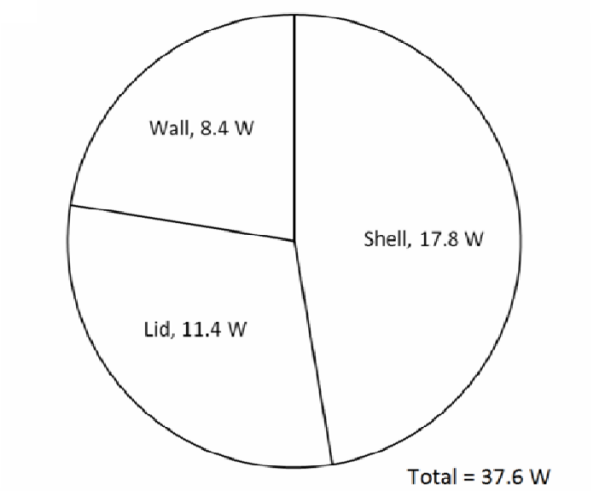

Fig. 7. Calculated heat leak into transformer cryostat. Note: that the pie chart area scale is identical to that in Fig. 6.

B. AC loss in Roebel cable winding

Fig. 8 shows AC loss measurements at 77 K at frequencies of 61.90, 43.73, and 35.70 Hz dictated by the coupling capacitances of 50, 100, and 150 µF used to connect the audio amplifier to the HV winding. The loss per cycle is the same for all three frequencies confirming that the loss is hysteretic as expected. The transport loss measured on a short sample of cable is plotted for comparison. To make allowance for the lower critical current of the transport loss sample (1200 A against 1420 A for the LV winding cable length) we assume scaling of transport loss

$$Q \propto I_c^2 \cdot f\left(\frac{I}{I_c}\right) \qquad (2)$$

to calculate what the transport loss would be if the sample I_c was 1420 A. The coil loss and transport loss have very similar power law dependence on current amplitude, with a power law exponent of 3.35 at 800 A. The coil loss is about 80% greater than the scaled transport loss. The measured coil loss becomes progressively less than the prediction of the Norris strip model [16] at current amplitudes above about 1/3 of I_c.

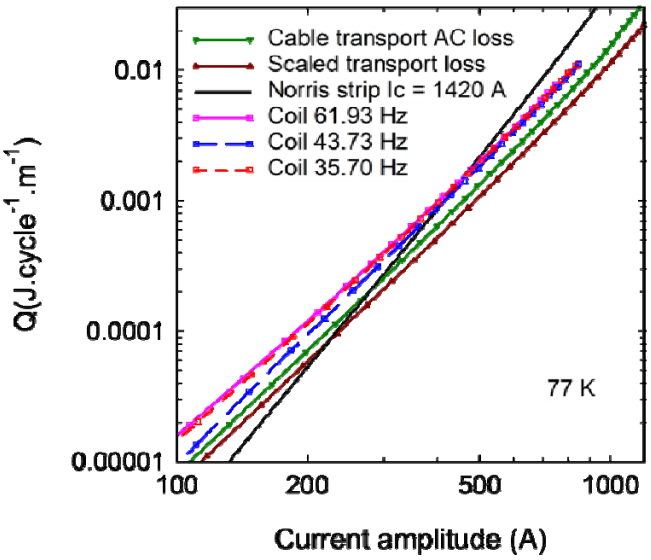

Fig. 8 AC loss in the LV winding at 77 K compared with transport loss before and after scaling to allow for difference in critical currents.

Fig. 9 shows the AC loss of the LV winding measured at 70.5 K at a frequency of 35.7 Hz. This shows that the AC loss of the winding at the rated current of 1390 A rms at 50 Hz will be 130 W. At 50% of rated current this drops to 8.5 W. At rated current the measured loss is about 60% of the Norris strip prediction calculated using a critical current estimated from cable strand $I_c(B)$ data using a load-line method [9]

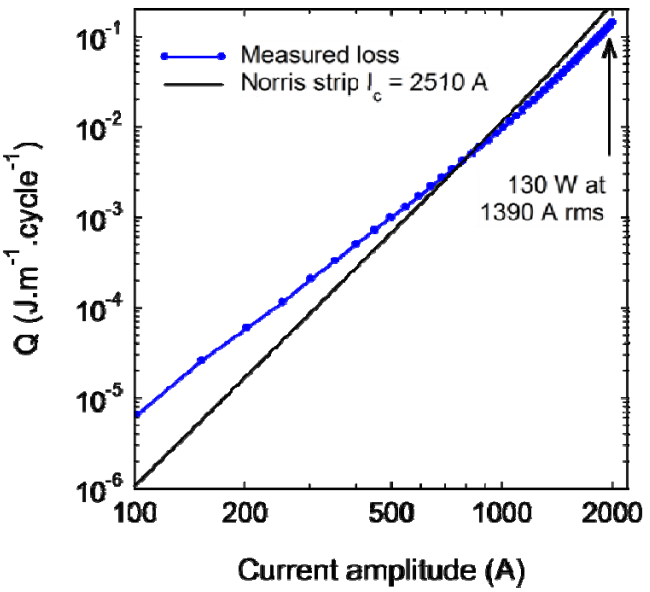

Fig. 9. AC loss of the LV winding measured at 70.5 K

C. Prediction of total cryogenic heat load

We can apply the values above for cryostat performance and AC loss in the LV winding, combined with earlier predictions for AC loss in the HV winding and electrical bushings to establish a prediction of total heat load on the

cryogenic space. This prediction is summarized in Table III. This indicates that the contribution from AC loss is about equal to that from cryostat and electrical bushing losses combined. It is important to realize that the transformer design presented here is particularly challenging to achieve efficiency approaching that of conventional transformer technology of the same rating. The electrical efficiency (considering only AC loss) is very good at 99.95%, but for a valid comparison we must apply a realistic cooling penalty of say 30:1 (30 W of energy to remove 1 W of heat from the cold space). Thus the overall efficiency of our 1 MVA transformer is expected to be closer to 97%. Current efficiency standards for a transformer of this rating stipulate a minimum efficiency of 99.27% - when measured at 50% of rated load [14]. Estimating AC loss at 50% of rated load produces a comparative efficiency value of about 98.5% for the HTS transformer – still somewhat short of the efficiency already attained with conventional technology.

TABLE III
PREDICTED HEAT LOAD ON CRYOGENIC SPACE AT RATED CURRENT

Source	Heat load (W)
Cryostat	113
Electrical bushings [13]	343
AC loss in LV [12]	390
AC loss in HV	90
Total	936

To achieve an HTS transformer with considerably higher efficiency, we consider that a commercially viable transformer will have a much higher rating and operate at higher voltages. For example a 10 MVA 66kV – 11kV transformer will have lower current electrical bushings (so reduced heat leak via this path), and marginally higher cryostat heat leak. AC loss can be expected to scale with conductor length.

IV. SUMMARY

We have presented results from experiments to determine the heat leak into the cryostat, and to accurately predict the AC loss we can expect in the Roebel cable winding of a demonstration 1 MVA three phase transformer. The predicted electrical efficiency is very good but the combined heat loads, factored by the cooling penalty associated with extracting heat from a cryogenic environment, mean that the overall efficiency of the transformer is somewhat less than existing transformer standards specify.

The future potential for a practical HTS transformer lies in higher rated and higher voltage machines, but our current project is a valuable demonstration of a particularly challenging application for HTS conductors – proving the advantages offered by Roebel cable technology in high current AC windings. Utilising 2G-HTS Roebel cable, AC loss is not a fundamental obstacle to HTS transformer commercialisation.

ACKNOWLEDGMENT

IRL thanks the industry partners for their valued contributions to this project: Wilson Transformer Company, ETEL, Vector, General Cable Superconductors and HTS-110.

This work was supported in part by the New Zealand Ministry of Business, Innovation and Employment under TRST contract C08X0818.

REFERENCES

[1] N. J. Long R. Badcock, P. Beck, M. Mulholland, N. Ross, M. Staines, H. Sun, J. Hamilton and R. G. Buckley "Narrow Strand YBCO Roebel Cable for Lowered AC Loss", *IEEE/CSC & ESAS European Superconductivity News Forum,* no. 3. January 2008

[2] W. Goldacker, A. Frank, A. Kudymow, R. Heller, A. Kling, S. Terzieva, and C. Schmidt, "Status of high transport current ROEBEL assembled coated conductor cables," *Supercond. Sci. Technol.*, vol. 22, pp. 034003. 2009.

[3] Z. Jiang, K. P. Thakur, N. J. Long, R. A. Badcock, M. P. Staines, "Comparison of transport AC losses in an eight-strand YBCO Roebel cable and a four-tape YBCO stack," *Physica. C, Superconductivity and its applications* Vol. 471, no. 21-22, pp. 999-1002. 2011.

[4] N. J. Long, R. A. Badcock, K. Hamilton, A. Wright, Z. Jiang, L. S. Lakshmi, "Development of YBCO Roebel cables for high current transport and low AC loss applications," (2010) Journal of Physics: Conference Series, Vol. 234 (Part 2), art. no. 022021. 2010.

[5] S. S. Kalsi, *Applications of high temperature superconductors to electric power equipment.* New Jersey: Wiley; 2011.

[6] E. F. Pleva, V. Mehrotra, S. W. Schwenterly, "Conductor requirements for high-temperature superconducting utility power transformers." *Supercond. Sci. Technol.* 23 (2010) 014025 (5pp)

[7] J. P. Sass, W. W. St.Cyr, T. M. Barrett, R. G. Baumgartner, J. W. Lott, and J. E. Fesmire. " Glass bubbles insulation for liquid hydrogen storage tanks," *Advances in Cryogenic Engineering: Transactions of the Cryogenic Engineering Conference CEC,* Vol. 55, pp. 772 – 779. 2009.

[8] S. W. Schwenterly, Y. Zhang, E. F. Pleva and M. Rufer "Vacuum studies of a prototype composite coil dewar for HTSC transformers", *Advances in Cryogenic Engineering: Transactions of the Cryogenic Engineering Conference CEC,* Vol 55, pp. 764 – 771. 2009.

[9] M. P. Staines, N. D. Glasson, M. Pannu, K. P. Thakur, R. A. Badcock, N. Allpress, P. D'Souza, and E. Talantsev. "The development of a Roebel cable based 1 MVA HTS transformer." *Superconductor Science and Technology,* Vol. 25. 2012.

[10] http://cryogenics.nist.gov/MPropsMAY/materialproperties.htm

[11] B. E. Scholtens, J. E. Fesmire, J. P. Sass, S. D. Augustynowicz, and K. W. Heckle "Cryogenic thermal performance testing of bulk-fill and aerogel insulation materials", *Advances in Cryogenic Engineering: Transactions of the Cryogenic Engineering Conference CEC,* Vol 53 pp. 152 – 159. 2007

[12] N. D. Glasson, M. P. Staines, R. G. Buckley, M. Pannu, S. S. Kalsi, "Development of a 1 MVA 3-Phase Superconducting Transformer using YBCO Roebel Cable," *IEEE transactions on Applied Superconductivity,* Vol. 21, No. 3 pp. 1393 – 1396. 2011.

[13] R. McFee, "Optimum input leads for cryogenic applications," *The review of scientific instruments."* Vol. 30, No. 2, 1959.

[14] AS2374.1.2-2003 Power transformers part 1.2: Minimum energy performance standard (MEPS) requirements for distribution transformers.

[15] J. Souc, F. Gömöry, and M. Vojenčiak, "Calibration free method for measurement of the AC magnetization loss," *Superconductor Science and Technology,* Vol. 18, No. 5. pp 592-595, 2005.

[16] W. T. Norris, "Calculation of hysteresis losses in hard superconductors carrying a.c.: isolated conductors and edges of thin sheets", *J Phys. D.*, 3, pp 486-507, 1970.